Catalysis Today 157 (2010) 2–7

Contents lists available at ScienceDirect

Catalysis Today

journal homepage: www.elsevier.com/locate/cattod

Atomic aspects of surface chemical reactions

Kiyotaka Asakura *

Catalysis Research Center, Hokkaido University, Kita-ku Kita 21-10, Sapporo 001-0021, Japan

ARTICLE INFO

Article history:
Available online 16 February 2010

Keywords:
Surface science
Pressure gap
Material gap
Artificial control of reaction
Synthesis of surface structure
PTRF-XAFS

ABSTRACT

Developments in surface science have provided atomic-scale surface images and helped us to understand surface reactions at an atomic-scale. Two big gaps, the pressure gap and material gap, were believed to exist between real catalyst systems and surface science targets; however, they are now being filled. Nonlinear optical phenomenon of sum-frequency generation, glancing-angle X-ray, and scanning probe techniques have been developed as ambient pressure surface analysis methods. Great efforts have made it possible to perform X-ray photoelectron spectroscopy measurements in the presence of gas-phase reactants. Recent improvements in surface analysis techniques for nonconducting targets enable us to investigate metal clusters on well-defined oxide surfaces to fill the material gap. We are now able to initiate and control the surface reactions artificially by adjusting physical parameters. Surface science has reached a new stage not only for determining the surface structures, electronic properties, and reaction mechanisms but also for synthesizing highly active surfaces and controlling catalytic reactions artificially.

© 2010 Elsevier B.V. All rights reserved.

1. Introduction

Recent developments in surface science techniques have provided atomic-scale surface images and confirmed our understanding of surface phenomena at the atomic and molecular scales. Modern surface science is based on three techniques:

1. Electron analysis such as low-energy electron diffraction (LEED), reflection high-energy electron diffraction (RHEED), high-resolution electron energy loss spectroscopy (HREELS), X-ray photoelectron diffraction (XPD), ultraviolet photoelectron spectroscopy (UPS), and X-ray photoelectron spectroscopy (XPS), which are surface-sensitive due to the electron's small escape depth from the material [1].
2. Preparation and characterization of well-defined single-crystal surfaces.
3. The ultrahigh vacuum (UHV) technique.

Despite great success of surface science, gaps are believed to exist between surface science and real catalytic systems [2], namely, the "pressure gap" and "material gap". Many surface science techniques require UHV conditions, while practical catalytic reactions occur at ambient pressure or pressures higher than 1 atm. Thus, differences in the order of 10^{13} exist between surface science and real catalytic systems; this difference is called the pressure gap. The material gap exists because surface science uses well-defined flat surfaces to decrease complexity whereas practical catalyses occur on inhomogeneous, complex materials that are highly porous and composed of multiple elements and phases to increase the activities and selectivities.

Recently, challenges have been addressed to fill these gaps [2]. In this plenary talk, I review some examples of the attempts to fill the pressure and material gaps in oxidation catalysts. In the last Section, I will discuss the future of surface science in oxidation reactions, focusing on the possibility of fine synthesis of highly active surface structure and artificial control of surface reactions, which are the greatest advantages of surface science.

2. To overcome the pressure gap

Surface science requires UHV conditions because a clean surface is rapidly contaminated unless the UHV condition is satisfied and also because electrons are easily scattered by gas-phase components. The pressure gap has been filled by changing the characterization and reaction conditions. Once a clean, well-defined surface is prepared and characterized by surface science techniques, the reaction can then be performed under ambient conditions. Somorjai and Goodman revealed the structural dependence of the reactivities of single-crystal surfaces using this method [3,4]. Nowadays the surface characterization can be carried out in the presence of gas-phase in two ways. One is to use surface-sensitive techniques other than electron spectroscopy, such as scanning probe techniques and photon spectroscopy. The other is to reduce the scattering of electrons by the gas-phase.

* Fax: +81 11 706 9113.
E-mail address: askr@cat.hokudai.ac.jp.

0920-5861/$ – see front matter © 2010 Elsevier B.V. All rights reserved.
doi:10.1016/j.cattod.2010.01.024

STM does not require high vacuum in its measurement. Fig. 1a shows the TiO_2(1 1 0) surface structure [5]. Big and small filled balls are oxygen and Ti atoms, respectively. Protruding oxygen atoms (called bridging oxygen) are arranged in a row along the [0 0 1] direction, while the 5-fold Ti atoms exposed to the surface are arranged in a row parallel to the [0 0 1] direction. Fig. 1b and c shows scanning tunneling microscopy (STM) images of the clean TiO_2(1 1 0) and the CH_3COOH adsorbed surfaces, respectively [6]. The bright spots in Fig. 1b make a line corresponding to the 5-fold Ti atoms, and the dark bands between the bright lines correspond to protruding oxygen atoms that are in the [0 0 1] direction. Note that STM can observe Ti atoms due to the electronic effect although Ti atoms are below the protruding oxygen atoms [5]. Bright spots in the dark bands correspond to oxygen defects or OH groups that have a large tunneling probability. When TiO_2(1 1 0) is exposed to CH_3COOH, the CH_3COOH is dissociatively adsorbed on two 5-fold Ti atoms to form a bridging acetate. The adsorbed acetates form a uniform lattice structure with twice the periodicity of the substrate in the [0 0 1] direction (2×1 structure), as shown in Fig. 1c. STM can provide atomic-scale images of surfaces that show surface defects and adsorbates. Henderson et al. observed the photo-decomposition reaction of trimethylacetate in the presence of oxygen and discussed the role of oxygen [7]. Aizawa et al. revealed the formate decomposition reaction on the TiO_2(1 1 0) surface. They concluded that the monodentate formate species was the reaction intermediate for the decomposition reaction [8,9].

Photon is not as strongly affected by the presence of the gas-phase. Reflection-absorption infrared spectroscopy (RAIRS) can provide surface vibrational information about the adsorbate [10]. To distinguish the surface adsorbate and gas-phase signals, polarization-modulated RAIRS (PM-RAIRS) is adopted, because the adsorbate vibrational mode absorbs only p-polarized light, whereas the gas-phase can absorb both p- and s-polarized lights. When the difference spectra are taken between both p- and s-polarized lights, one may remove the gas-phase effect and obtain surface-sensitive information. Sum-frequency generation (SFG) is a more surface-sensitive technique, because its signal arises only from the surface region where no inversion center exists. Rupprechter et al. studied CO, CH_3OH, and CH_4 oxidation reactions under ambient pressure by PM-RAIRS and SFG [11–13].

X-ray diffraction, scattering, and absorption can yield structural information. However, X-ray can penetrate deeply into the material and are not usually surface-sensitive. When a flat surface is used and X-ray hits the surface at a grazing-angle or at an incident angle less than the critical angle, δ_c (normally 10 mrad), total reflection of the X-ray occurs. In this case, the X-ray cannot penetrate deeply into the bulk of the material (penetration depth $<$ a few nm), and X-ray become surface-sensitive [14]. Thus, grazing-angle X-ray diffraction reveals the surface lattice structure more precisely than LEED, because the latter suffers from multiple scattering. Relaxation of the TiO_2(1 1 0) surface was determined by surface X-ray diffraction techniques [15,16]. The bridging oxygen and 5-fold Ti are relaxed upward by 0.010 nm and downward by 0.011 nm [16]. In the next section, I will discuss polarization-dependent total reflection fluorescence X-ray absorption fine structure spectroscopy (PTRF-XAFS), which is suitable for structural analysis of metal species that is highly dispersed on a flat substrate [17–19].

In order to reduce the scattering of electrons by the gas-phase components the energy analyzer is placed close to the sample and is differentially pumped. Fig. 2 shows a schematic drawing of the ambient XPS [20]. A photoelectron excited by X-ray goes into the XPS instrument. Electron lenses placed before the energy analyzer collect the ejected electrons at focal points. Apertures are placed at these focal points so that differential pumping becomes possible before and after the apertures without loss of photoelectrons. Consequently, the pressure around the sample can be maintained high ($>$1 mbar) while the XPS analyzer is under high vacuum [21–25]. Atop CO, which had never been observed under high vacuum, was observed at 286.6 eV in the presence of 1 mbar CO by the ambient XPS [26].

The desorption angle and translational energy analysis of the reaction products can yield reaction site information if the product suffers repulsive interaction from the surface, as CO_2 does [27]. Matsushima et al. intensively studied the angular distribution of the CO oxidation reaction. CO oxidation occurs via the

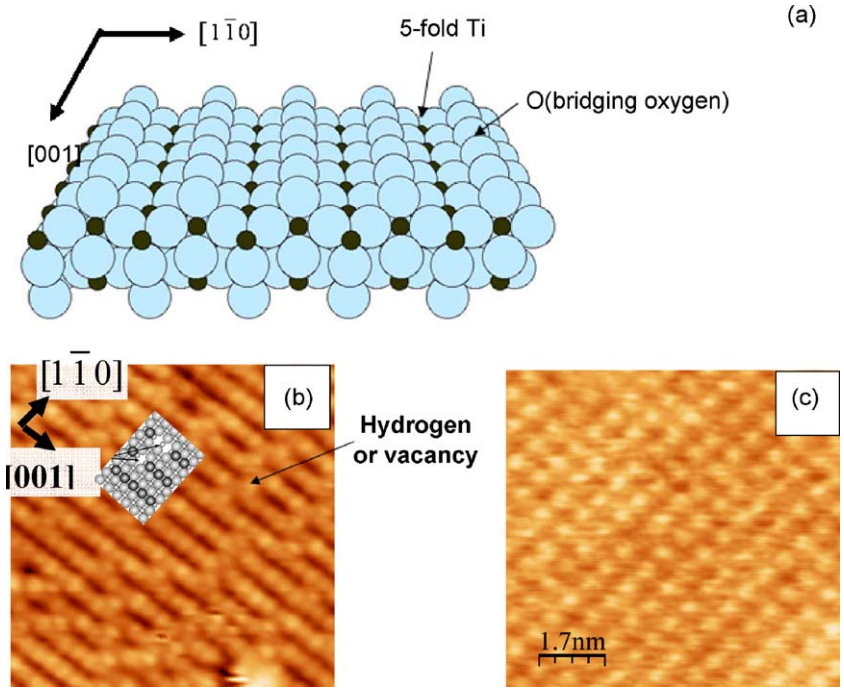

Fig. 1. (a) TiO_2(1 1 0) surface; large and small filled balls are oxygen and Ti atoms, respectively. (b) STM image of clean TiO_2(1 1 0) surface. (c) STM image of CH_3COOH-adsorbed TiO_2(1 1 0).

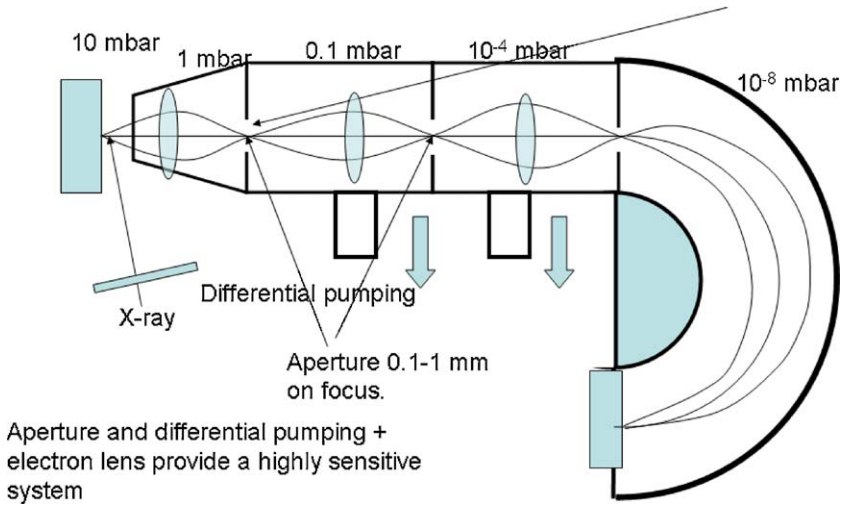

Fig. 2. Schematic drawing of ambient XPS system.

Langmuir–Hinshelwood mechanism, in which both adsorbed CO and oxygen react on the surface. CO_2 desorption occurs mainly along the perpendicular direction of the Pd(1 1 0) surface after the CO oxidation reaction. The angular distributions along [1 $\bar{1}$ 0] and [0 0 1] are proportional to $\cos^3\theta$ and $\cos^{10}\theta$, respectively, at 420 K, indicating that the CO_2 desorption distribution is sharp along [0 0 1] and wide in the [1 $\bar{1}$ 0] direction [27]. Here, θ is defined as the angle between the desorption direction and surface normal. This result implies that the CO oxidation reaction takes place at the valley Pd atoms between the Pd ranges running along the [1 $\bar{1}$ 0] direction. Infrared emission spectroscopy of the desorbed gas can provide information about the vibrational and rotational states of the desorbed products [28,29], which conveys the structure of the reaction intermediate. If CO and oxygen react in a head-on manner as shown in Fig. 3a, the antisymmetric vibrational mode is excited; if they react in a side-on manner as shown in Fig. 3b, the bending and rotational modes are excited in addition to the antisymmetric mode. Nakao and Kunimori revealed that the CO oxidation reaction on Pd(1 1 1) goes with a side-on collision at high temperature, while it occurs in a rather head-on manner at low temperature [30,31]. If the vibrational and rotational modes of the desorbed products are identified in an angle-resolved way, one can determine the shape of the reaction intermediate and detail the reaction mechanism as well as the reaction site structure. However, the signal of angle-resolved infrared emission is too small and is obscured by background infrared emission. Thus, the angle-resolved infrared emission spectroscopy of desorbed products is extremely difficult. Yamanaka addressed this difficulty by cooling the entire system to a liquid N_2 temperature and successfully measured the angle-resolved infrared emission [32–34]. The intermediate state of CO_2 on Pd(1 1 1) at 700 K is produced through a side-on interaction between O and CO and has a molecular alignment with its molecular axis parallel to the surface. The angle-resolved infrared emission provides a more detailed view of the surface intermediate. In normal desorption direction, the bending mode of the desorbed CO_2 is excited, as shown in Fig. 3c, while the rotational mode is not excited. In the off-normal direction, the rotational mode is rather excited, but bending mode excitation decreases (Fig. 3c). Prior to desorption, the CO_2 is bound to the surface through two bonds at O and C(O). If the O–substrate bond is cleaved first, the rotationally excited CO_2 is desorbed in the off-normal direction. On the other hand, if the C(O)–substrate bond is first cleaved, the CO_2 is desorbed mainly in the normal direction with the highly excited bending mode.

3. To fill the material gap

The largest difference between real systems and single-crystal surfaces appears in the supported metal catalysts. A real system is composed of nanoclusters with different surface structures involving corners and steps supported on a porous inorganic oxide, whereas a single-crystal system is basically flat. Periodic steps can be prepared on single-crystal surfaces, but the nanoscale particle size affects the catalyses tremendously, as found in Au nanoparticles [35]. The deposition of metal on a flat metal oxide surface gives a model supported catalyst system. When the oxide surface has an electrical conductivity, STM can reveal the size and morphology of nanoparticles deposited on the surface. However, many oxides, such as MgO, SiO_2, and Al_2O_3, are insulators and hence we cannot directly observe the oxide surface by STM. The preparation of a well-defined oxide thin film on a metallic substrate is one way to observe an oxide surface by STM [36]. Sterrer prepared a MgO(1 0 0) thin film on a Ag(1 0 0) surface and observed the defects present in the MgO(1 0 0) surface. The defect energy levels depend on their locations [37]. An Al_2O_3 thin film has been grown on a surface by the oxidation of NiAl(1 1 0) [38]. A SiO_2 thin film grown on Mo(1 1 2) has an isolated structure linked to the Mo surface through a Si–O–Mo bond [39–41]. A TiO_2 thin film can be grown on Mo(1 1 2) to yield a well-ordered (8×2) structure [41–43]. Chen and Goodman revealed that two-monolayer Au deposited on TiO_2/Mo showed very high activity for the CO oxidation reaction [43]. The other way to observe an oxide surface is to use non-contact atomic force microscopy (NC-AFM), which does not require electrical conductivity and has been used in the MoO_3, NiO, CeO_2, Al_2O_3, and TiO_2 surfaces [44–51]. Recently, ambient-condition STM and AFM have been applied to surface science studies [52–54]. An NC-AFM study on Au on fully oxidized TiO_2(1 1 0) showed high Au mobility under the presence of air at room temperature, while Au particles were immobile under a high vacuum [54].

When Ni is deposited on the TiO_2(1 1 0) surface, surface Ni clusters of a certain size are produced at lower coverage (0.03 ML), as shown in Fig. 4; the number of Ni clusters with a certain size increases with further deposition of Ni. We call such a deposition mode of Ni on TiO_2(1 1 0) a self-regulated growth mode [55]. The interaction between the Ni clusters and TiO_2(1 1 0) surface may stabilize clusters of a specific size and initiate the self-regulated growth mode. However, atomic-scale information about the interaction between Ni clusters and the substrate is lacking in STM observations. XAFS spectroscopy yields structural

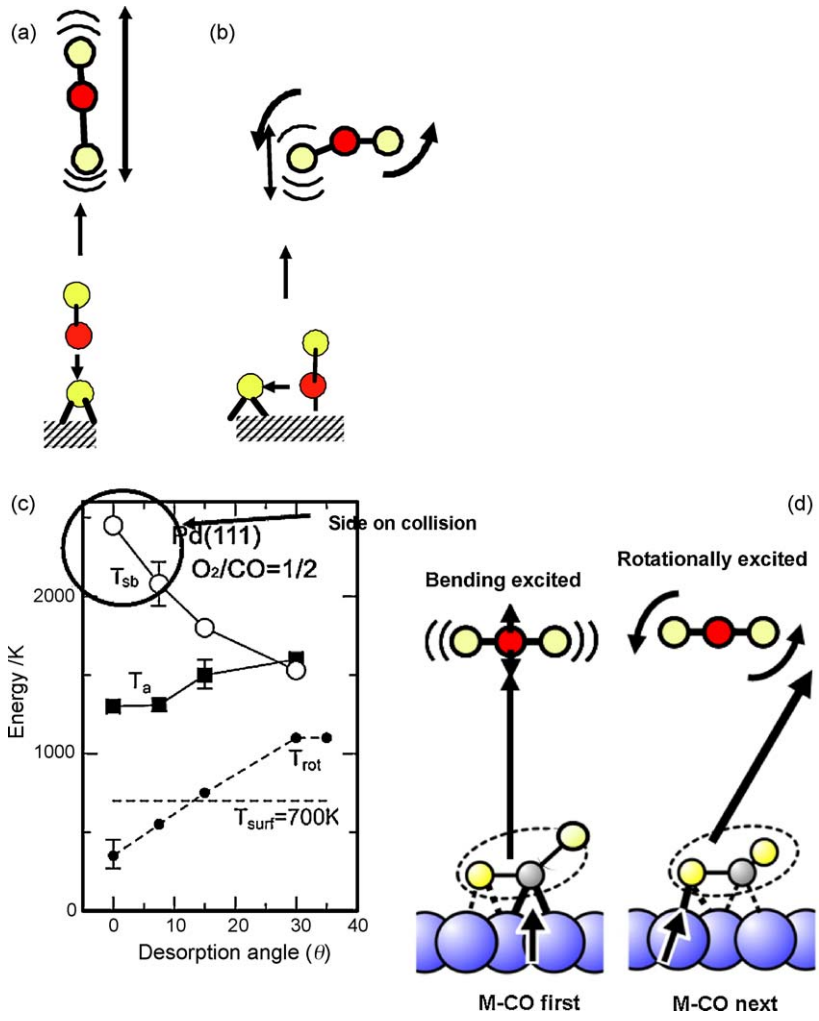

Fig. 3. Vibrational and rotational states of desorbed CO_2 after CO oxidation reaction. (a) Oxygen atom collides with CO head-on. (b) Oxygen atom collides with CO side-on. (c) Desorption angular dependency of energy states for vibrational and rotational modes of desorbed CO_2. The energy is expressed by the temperature. (d) Schematic explanation of desorption direction and excitation mode.

information around the X-ray absorbing atom [56]. The XAFS intensity has X-ray polarization dependence. When the angle between the X-ray electric vector and the bond direction is defined as θ, XAFS intensity is proportional to $3\cos^2\theta$. When metal particles are deposited on a flat oxide substrate system and the polarization direction is set parallel to the oxide surface, the XAFS signal of the deposited metal is dominated by the metal–metal interaction, as shown in Fig. 4b. When it is set normal to the surface, the metal–substrate structure is mainly elucidated as shown in Fig. 4c. PTRF-XAFS has been applied to Ni clusters on the TiO_2(1 1 0) surface to

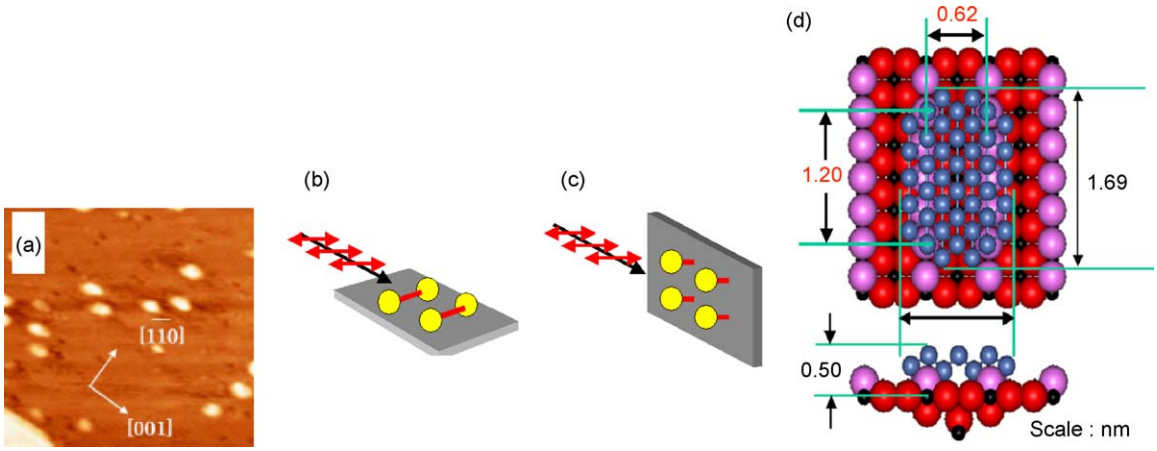

Fig. 4. (a) STM image of Ni clusters on TiO_2(1 1 0) surface. Ni coverage is 0.03 ML. (b) and (c) indicate the polarization direction and the information about bond given by PTRF-XAFS, respectively. (d) Model structure for Ni clusters on TiO_2(1 1 0) surface.

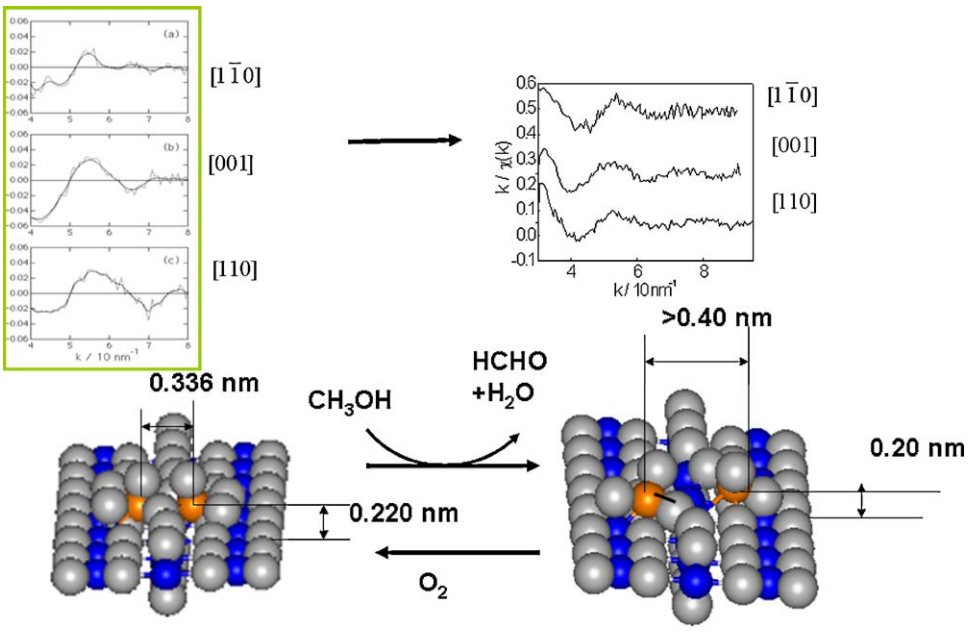

Fig. 5. Upper panel: PTRF-XAFS oscillations for Mo dimers after oxidation reaction (upper left) and Mo monomers after the reaction with CH_3OH (upper right). Lower panel: schematic drawing of the structural change during the reaction.

clarify the self-regulated growth mechanism [57–59]. The Ni clusters are found with a structure shown in Fig. 4d, where 86% of the Ni atoms in the cluster bond with the protruding oxygen atoms of the TiO_2(1 1 0) surface thus stabilizing the surface cluster structure. Such interaction between metal clusters and protruding oxygen atoms was found in a Cu cluster on the TiO_2(1 1 0) surface [60]. PTRF-XAFS can provide information about structural change during the reaction because X-rays can go through the gas-phase. Mo dimers are created on the TiO_2(1 1 0) surface and they catalyze the CH_3OH oxidation reaction [17,61–65]. In situ PTRF-XAFS under the oxidation reaction reveals that the reaction takes place by the Mars–van Krevelen mechanism in which the Mo dimer structure is broken by the reaction with CH_3OH and is regenerated after the oxidation process, as shown in Fig. 5.

4. The future of surface science in catalysis: synthesis of highly active structures and artificial control of surface reactions

The flat substrate has the advantages of easy characterization and easy-to-control preparation. The above developments in surface science have made it possible to perform in situ surface characterization under reaction conditions. The disadvantages of the flat surface could be low surface area and low activity. However, if one can precisely synthesize a highly active surface species it will be the most efficient catalyst. Hara et al. prepared a well-defined Pd complex on the Si(1 1 1) surface linked with bisoxazoline molecules and demonstrated the possibility of synthesizing a highly active species on a flat surface [66–68]. A small Si tip (5 mm × 5 mm) with the Pd complex converted benzyl alcohols to benzyl aldehyde by gas-phase oxygen atoms with nearly 100% conversion and TON = 410,000. Lithographic techniques that have been successful in the fabrication of electronic devices can be applied to surface science preparation of well-defined inhomogeneous surfaces [69–71]. VSbO catalyst undergoes selective ammoxidation of propane [72]. A remote control mechanism is proposed for selective oxidation in which the oxygen activated in the Sb_2O_4 phase diffuses to the $VSbO_4$ surface and is used for the selective oxidation reaction [73]. The size and arrangement of the $VSbO_4$ and Sb_2O_4 phases are finely adjusted lithographically [74]. Fig. 6 shows preliminary results on the dependence of propene selective oxidation activity on the separation of Sb_2O_4 lines [75]. The width and separation of Sb_2O_4 lines are designed by lithography, maintaining the total surface areas of $VSbO_4$ and Sb_2O_4 constant, as shown in Fig. 6a. An optimum separation of Sb_2O_4 lines in this reaction exists, as shown in Fig. 6b, indicating that reaction control in the micrometer or submicrometer size created by lithography may be possible.

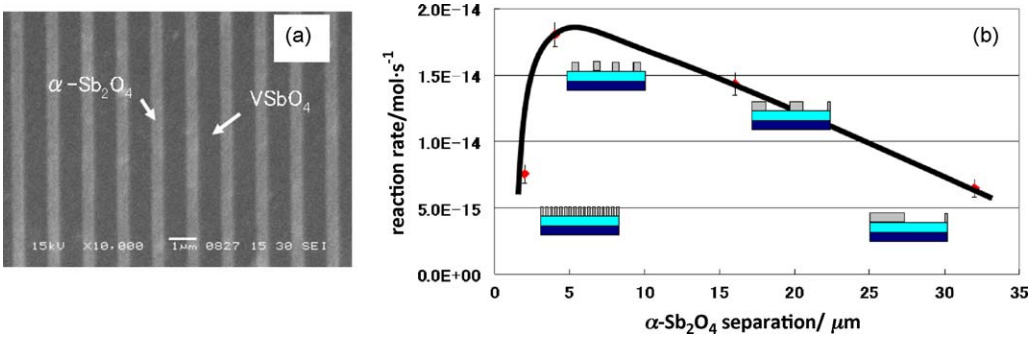

Fig. 6. SEM picture of lithographic Sb_2O_4–$VSbO_4$ surfaces (a) and acrolein formation activity dependence on the separation of Sb_2O_4 lines (b). 2.5×10^{-3} Pa C_3H_6 and 7.5×10^{-3} Pa O_2 are reacted on the surface at a temperature of 673 K.

The other advantage of using a flat surface is in controlling the catalytic reaction with in situ monitoring of the reaction and giving external impulses such as light, electric potential, and reactant pressure at an appropriate time and place. Rotermund et al. successfully controlled and modified the CO oxidation reaction pattern by the laser light [76–79]. A pulse infrared laser can control the surface reaction not only through a temperature increase but also through selective excitation of a specific vibrational mode. MoO_3 has five Mo–O bonds with different vibrational modes. An infrared laser emitted from a free electron laser system tuned to a specific vibrational bond (965 cm^{-1}) can initiate the C_2H_5OH decomposition reaction although no reaction occurs when the wavelength of the infrared laser is detuned from the vibrational mode [80,81].

5. Conclusions

Surface science has reached a new stage not only for determining the surface structure, electronic properties, and reaction mechanisms but also for synthesizing highly active surface species with a precise structure and controlling the catalytic reaction artificially. For this purpose, surface science will progress in cooperation with fine chemical syntheses, semiconductor device fabrication methods, laser and molecular beam technologies, and colloidal chemistry as well as by the improvement in its original methods.

Acknowledgments

The author expresses his thanks for the Grant-in-Aid for Scientific Research from the Japanese Scientific Promotion Society (JSPS) (No. 16106010) and to the Global COE Program of the Ministry of Education, Science and Technology of Japan. He thanks Prof. Y. Iwasawa (The Communication University of Tokyo), Prof. W.-J. Chun (ICU), Prof. S. Suzuki (Nagoya University), and Prof. S. Takakusagi, Prof. K. Hara, and Prof. T. Yamanaka (Catalysis Research Center, Hokkaido University) for kind and fruitful discussions.

References

[1] D.P. Woodruff, T.A. Delchar, Modern Techniques of Surface Science, Cambridge University Press, Cambridge, 1994
[2] R.T. Vang, E. Laegsgaard, F. Besenbacher, Phys. Chem. Chem. Phys. 9 (2007) 3460.
[3] G.A. Somorjai, Surface Chemistry, Wiley Interscience, New York, 1993.
[4] D.W. Goodman, Acc. Chem. Res. 17 (1984) 194.
[5] U. Diebold, Surf. Sci. Rep. 48 (2003) 53.
[6] K. Kinoshita, Surface Structure Determinations of Single Crystal Transition Metal Compound Model Catalysts, Hokkaido University, Sapporo, 2008, p. 122.
[7] M.A. Henderson, J.M. White, H. Uetska, H. Onishi, J. Catal. 238 (2006) 153.
[8] Y. Morikawa, I. Takahashi, M. Aizawa, Y. Namai, T. Sasaki, Y. Iwasawa, J. Phys. Chem. B 108 (2004) 14446.
[9] M. Aizawa, Y. Morikawa, Y. Namai, H. Morikawa, Y. Iwasawa, J. Phys. Chem. B 109 (2005) 18831.
[10] J.T. Yates Jr., T.E. Madey, Vibrational Spectrsocopy of Molecules on Surfaces, Prenum Press, New York, 1987.
[11] G. Rupprechter, C. Weilach, J. Phys.: Condens. Matter 20 (2008) 184020.
[12] G. Rupprechter, Catal. Today 126 (2007) 3.
[13] M. Baumer, J. Libuda, K.M. Neyman, N. Rosch, G. Rupprechter, H.J. Freund, Phys. Chem. Chem. Phys. 9 (2007) 3541.
[14] T. Ohta, K. Asakura, T. Yokoyama, in: H. Saisho, Y. Gohshi (Eds.), Applications of Synchrotron Radiation to Materials Analysis, Amsterdam, 1996, p. 307.
[15] G. Charlton, P.B. Howes, C.L. Nicklin, P. Steadman, J.S.G. Taylor, C.A. Muryn, S.P. Harte, J. Mercer, R. McGrath, D. Norman, T.S. Turner, G. Thornton, Phys. Rev. Lett. 78 (1997) 495.
[16] G. Cabailh, X. Torrelles, R. Lindsay, O. Bikondoa, I. Joumard, J. Zegenhagen, G. Thornton, Phys. Rev. B 75 (2007).
[17] K. Asakura, W.J. Chun, Y. Iwasawa, Top. Catal. 10 (2000) 209.
[18] M. Shirai, T. Inoue, H. Onishi, K. Asakura, Y. Iwasawa, J. Catal. 145 (1994) 159.
[19] W.J. Chun, Y. Tanizawa, T. Shido, Y. Iwasawa, M. Nomura, K. Asakura, J. Synchrotron Radiat. 8 (2001) 168.
[20] M. Salmeron, R. Schlogl, Surf. Sci. Rep. 63 (2008) 169.
[21] E. Kleimenov, H. Bluhm, M. Havecker, A. Knop-Gericke, A. Pestryakov, D. Teschner, J.A. Lopez-Sanchez, J. Bartley, G.J. Hutchings, R. Schlogl, Surf. Sci. (2004).
[22] D. Teschner, A. Pestryakov, E. Kleimenov, M. Haevecker, H. Bluhm, H. Sauer, A. Knop-Gericke, R. Schlogl, J. Catal. 230 (2005) 195.
[23] J. Pantforder, S. Pollmann, J. Zhu, D. Borgmann, R. Denecke, H. Steinruck, Rev. Sci. Instrum. 76 (2005).
[24] M. Havecker, R.W. Mayer, A. Knop-Gericke, H. Bluhm, E. Kleimenov, A. Liskowski, D. Su, R. Follath, F.G. Requejo, D.F. Ogletree, M. Salmeron, J.A. Lopez-Sanchez, J. Bartley, G.J. Hutchings, R. Schlogl, J. Phys. Chem. B 107 (2003) 4587.
[25] R.W. Mayer, M. Havecker, A. Knop-Gericke, R. Schlogl, Catal. Lett. 74 (2001) 115.
[26] M. Kinne, T. Fuhrmann, C. Whelan, J. Zhu, J. Pantforder, M. Probst, G. Held, R. Denecke, H. Steinruck, J. Chem. Phys. 117 (2002) 10852.
[27] T. Matsushima, Surf. Sci. Rep. 52 (2003) 1.
[28] K. Nakao, S. Ito, K. Tomishige, K. Kunimori, J. Phys. Chem. B 109 (2005) 17553.
[29] K. Nakao, S. Ito, K. Tomishige, K. Kunimori, J. Phys. Chem. B 109 (2005) 17579.
[30] K. Nakao, H. Hayashi, H. Uetsuka, S. Ito, H. Onishi, K. Tomishige, K. Kunimori, Catal. Lett. 85 (2003) 213.
[31] K. Nakao, S.I. Ito, K. Tomishige, K. Kunimori, Catal. Today 111 (2006) 316.
[32] T. Yamanaka, T. Matsushima, Phys. Rev. Lett. 100 (2008) 026104.
[33] T. Yamanaka, T. Matsushima, Rev. Sci. Instrum. 78 (2007) 034105.
[34] T. Yamanaka, J. Chem. Phys. 128 (2008) 171102.
[35] M. Haruta, Gold Bull. 37 (2004) 27.
[36] M. Baumer, H.J. Freund, Prog. Surf. Sci. 61 (1999) 127.
[37] M. Sterrer, M. Heyde, M. Novicki, N. Nilius, T. Risse, H.P. Rust, G. Pacchioni, H.J. Freund, J. Phys. Chem. B 110 (2006) 46.
[38] A. Stierle, F. Renner, R. Streitel, H. Dosch, W. Drube, C. BC, Science 303 (2004) 1652.
[39] M.S. Chen, D.W. Goodman, Surf. Sci. 600 (2006) L255.
[40] S. Wendt, M. Frerichs, T. Wei, M.S. Chen, V. Kempter, D.W. Goodman, Surf. Sci. 565 (2004) 107.
[41] M.S. Chen, W.T. Wallace, D. Kumar, Z. Yan, K.K. Gath, Y. Cai, Y. Kuroda, D.W. Goodman, Surf. Sci. 581 (2005) L115.
[42] M.S. Chen, A.K. Santra, D.W. Goodman, J. Phys. Chem. B 108 (2004) 17940.
[43] M.S. Chen, D.W. Goodman, Science 306 (2004) 252.
[44] S. Morita, R. Wiesendanger, E. Meyer (Eds.), Non-contact Atomic Force Microscopy, Berlin, Springer, 2002.
[45] G.S. Enevoldsen, A.S. Foster, M.C. Christensen, J.V. Lauritsen, F. Besenbacher, Phys. Rev. B 76 (2007) 205415.
[46] C.L. Pang, A. Sasahara, H. Onishi, Q. Chen, G. Thornton, Phys. Rev. B 74 (2006) 073411.
[47] K. Fukui, Y. Iwasawa, Surf. Sci. Lett. 464 (2000) L719.
[48] M. Ashino, T. Uchihashi, K. Yokoyama, Y. Sugawara, S. Morita, M. Ishikawa, Phys. Rev. B 61 (2000) 13955.
[49] Y. Namai, K. Fukui, Y. Iwasawa, Nanotechnology 15 (2004) S49.
[50] H. Hosoi, K. Sueoka, K. Hayakawa, K. Mukasa, Appl. Surf. Sci. 157 (2000) 218.
[51] S. Suzuki, Y. Ohminami, T. Tsutsumi, M.M. Shoaib, M. Ichikawa, K. Asakura, Chem. Lett. 32 (2003) 1098.
[52] M. Montano, D.C. Tang, G.A. Somorjai, Catal. Lett. 107 (2006) 131.
[53] D.E. Starr, S.K. Shaikhutdinov, H.J. Freund, Top. Catal. 36 (2005) 33.
[54] S. Kielbassa, M. Kinne, R.J. Behm, J. Phys. Chem. B 108 (2004) 19184.
[55] K. Fujikawa, S. Suzuki, Y. Koike, W.-J. Chun, K. Asakura, Surf. Sci. 600 (2006) L117.
[56] Y. Iwasawa (Ed.), X-ray Absorption Fine Structure for Catalysts and Surfaces, World Scientific, Singapore, 1996.
[57] Y. Koike, K. Ijima, W.J. Chun, H. Ashima, T. Yamamoto, K. Fujikawa, S. Suzuki, Y. Iwasawa, M. Nomura, K. Asakura, Chem. Phys. Lett. 421 (2006) 27.
[58] Y. Koike, K. Fujikawa, S. Suzuki, W.J. Chun, K. Ijima, M. Nomura, Y. Iwasawa, K. Asakura, J. Phys. Chem. C 112 (2008) 4667.
[59] Y. Koike, W.J. Chun, K. Ijima, S. Suzuki, K. Asakura, Mater. Trans. 50 (2009) 509.
[60] Y. Tanizawa, T. Shido, Y. Iwasawa, M. Nomura, W.-J. Chun, K. Asakura, J. Phys. Chem. 107 (2003) 12917.
[61] W.J. Chun, K. Asakura, Y. Iwasawa, J. de Phys. 7-C2 (1997) 921.
[62] W.J. Chun, K. Asakura, Y. Iwasawa, Chem. Phys. Lett. 288 (1998) 868.
[63] W.J. Chun, K. Asakura, Y. Iwasawa, Catal. Today 44 (1998) 309.
[64] Y. Yamaguchi, W.J. Chun, S. Suzuki, H. Onishi, K. Asakura, Y. Iwasawa, Res. Chem. Intermediat. 24 (1998) 151.
[65] W.J. Chun, K. Asakura, Y. Iwasawa, Catal. Today 66 (2001) 97.
[66] G. Hamasaka, A. Ochida, K. Hara, M. Sawamura, Angew. Chem. Int. Ed. 46 (2007) 5381.
[67] K. Hara, K. Iwahashi, S. Takakusagi, K. Uosaki, M. Sawamura, Surf. Sci. 601 (2007) 5127.
[68] K. Hara, S. Tayama, H. Kano, T. Masuda, S. Takakusagi, T. Kondo, K. Uosaki, M. Sawamura, Chem. Commun. (2007) 4280.
[69] M.X. Yang, D.H. Gracias, P.W. Jacobs, G.A. Somorjai, Langmuir 14 (1998) 1458.
[70] M. Laurin, V. Johanek, A.W. Grant, B. Kasemo, J. Libuda, H.J. Freund, J. Chem. Phy. 122 (2005).
[71] M. Laurin, V. Johanek, A.W. Grant, B. Kasemo, J. Libuda, H.J. Freund, J. Chem. Phys. 123 (2005).
[72] G. Centi, S. Perathoner, Catal. Today 41 (1998) 457.
[73] B. Delmon, G.F. Froment, Catal. Rev. 38 (1996) 69.
[74] Y. Ohminami, S. Suzuki, N. Matsudaira, T. Nomura, W.J. Chun, K. Ijima, K. Nakamura, K. Mukasa, M. Nagase, K. Asakura, Bull. Chem. Soc. Jpn. 78 (2005) 435.
[75] T. Wada, S. Suzuki, M. Nakamura, K. Asakura, in press.
[76] J. Wolff, M. Stich, C. Beta, H.H. Rotermund, J. Phys. Chem. B 108 (2004) 14282.
[77] J. Wolff, H.H. Rotermund, New J. Phys. 5 (2003), 60.1.
[78] J. Wolff, A.G. Papathanasiou, H.H. Rotermund, G. Ertl, X. Li, I.G. Kevrekidis, J. Catal. 216 (2003) 246.
[79] J. Wolff, A.G. Papathanasiou, I.G. Kervekidis, H.H. Rotermund, G. Ertl, Science 294 (2001) 134.
[80] S. Sato, H. Niimi, S. Suzuki, W.-J. Chun, K. Irokawa, H. Kuroda, K. Asakura, Chem. Lett. 33 (2004) 558.
[81] M.G. Moula, S. Sato, K. Irokawa, H. Niimi, S. Suzuki, K. Asakura, H. Kuroda, Bull. Chem. Soc. Jpn. 81 (2008) 836.